Negative refraction and the spectral filtering of terahertz radiation by a photonic crystal prism

G. P. Swift,[1,2,*] A. J. Gallant,[2] N. Kaliteevskaya,[1,3] M. A. Kaliteevski,[1] S. Brand,[1] D. Dai,[1] A. J. Baragwanath,[1] I. Iorsh,[1] R. A. Abram,[1] and J. M. Chamberlain[1]

[1]*Department of Physics, Durham University, South Road, Durham, DH1 3LE, UK*

[2]*School of Engineering and Computing Sciences, Durham University, South Road, Durham, DH1 3LE, UK*

[3]*Ioffe Physical Technical Institute, 26 Polytekhnicheskaya, St. Petersburg 194021, Russia*

**Corresponding author: g.p.swift@durham.ac.uk*

Received January 5, 2011; revised March 14, 2011; accepted March 22, 2011; posted April 1, 2011 (Doc. ID 140067); published April 28, 2011

We demonstrate how micromachined photonic crystals can be used to negatively refract terahertz frequency light. The photonic crystals, which are constructed from conventional dielectric materials, manipulate the incident beam via interaction with their photonic bands. Consequently, we show that different components of a broadband beam incident on the structure may be positively or negatively refracted, depending upon its frequency and that the structure can be used as an effective spectral filter of THz radiation. © 2011 Optical Society of America

OCIS codes: 160.5293, 300.6495.

In recent years, advances in terahertz (THz) radiation techniques [1] have been applied to a wide variety of problems, including art conservation [2], biomedicine [3], and process control [4]. This has led to a demand for the development of components that can guide, focus, and filter THz radiation. Hence, as in optics more generally, there is a role for artificial optical materials that make possible negative refraction, where a refracted beam is on the same side of the normal to the interface as the incident beam [5]. The phenomenon of negative refraction was first theoretically proposed by Veselago in 1968 [6]. More recently, it has been observed in many systems, including those containing homogeneous materials [7], metamaterials based on split-ring resonators [8], and photonic crystals [9]. There has been intense interest in the phenomenon, because negatively refracting materials make possible new physical effects with many remarkable potential applications, including both the "superlens" [10] and the "cloak of invisibility" [11]. Since Isaac Newton first decomposed white light in 1667 [12], prisms have become a familiar optical tool, and in this Letter, we report an investigation of a prism that can cause both positive and negative refraction of THz radiation and, as a result, can provide exceptionally large angular dispersion of adjacent frequency bands.

For a material to have a negative refractive index, it must possess both a negative electromagnetic permeability and permittivity [6]. Recently, direct experimental evidence of the achievement of a negative refractive index at THz frequencies in a wedge-type metamaterial has been reported [13]. However, the condition of a negative refractive index is not necessary for the observation of negative refraction. The phenomenon of negative refraction simply requires that, in refraction at an interface, the refracted ray is on the same side of the normal as the incident ray; and this can occur, for example, at the surface of a conventional photonic crystal as a consequence of the nature of its band structure [14]. In this Letter, we show that strong negative refraction of THz radiation can be achieved at the surface of a simple metallic photonic crystal providing that its photonic band structure is suitably engineered [15]. Such photonic crystals are relatively easy to fabricate, and here we report measurements on a sample in the form of a prism, with particular attention to its potential as a spectral filter.

Micromachining can be used to produce three-dimensional structures (for example, pillars and holes) on a submicrometer to millimeter scale, dimensions that correspond to THz wavelengths. The technique is thus ideal for producing photonic devices that operate in the THz region of the electromagnetic spectrum. In recent work, we have shown how such devices can be used to filter THz radiation at normal incidence [16], and further theoretical developments of these ideas have considered waves that are obliquely incident on a prism structure of metallic pillars arranged on a hexagonal lattice [15]. The first two photonic bands of the basic hexagonal lattice system, with the electric field polarized parallel to the pillars' axis, are shown in Fig. 1(a); these

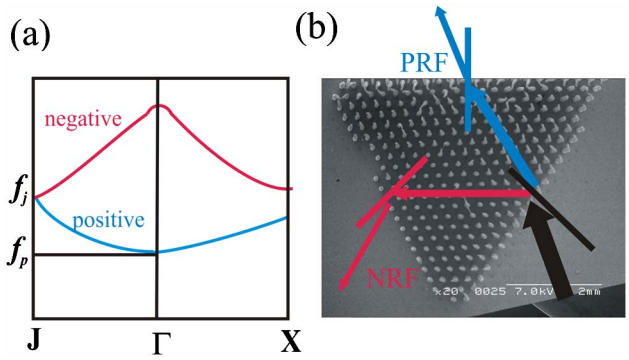

Fig. 1. (Color online) (a) Schematic diagram of the band structure of a photonic crystal having metallic pillars arranged on a hexagonal lattice. f_P and f_J denote the effective plasma frequency and frequency at the J symmetry point. If a wave with a frequency within the first band, lying between f_P and f_J, is incident on the prism, it should be positively refracted. On the other hand, if an incident wave has a frequency higher than f_J, and it lies within the second band, it should undergo negative refraction. (b) Scanning electron microscope image of the hexagonal metallic photonic crystal prism. The arrow on the right depicts the incident beam, while the arrows emerging from the surfaces labeled PRF and NRF show the directions of the positively and negatively refracted beams.

were obtained by employing the complex band structure method [17]. The structure possesses an effective plasma frequency, f_P, below which an electromagnetic wave cannot propagate, and a demarcation between the two bands occurs at the J point, at frequency f_J. The lowest band, with frequencies lying between f_P and f_J, is characterized by a group velocity parallel to the wave vector, but the second band, lying above f_J, is characterized by a group velocity antiparallel to the wave vector [15]. Because the group velocity of the transmitted wave must propagate into the medium, waves of frequency within the first band are positively refracted, while those in the second band are negatively refracted. Lower fill factors, and hence larger periods or smaller radii, reduce these frequencies, allowing devices to be developed that operate in differing frequency ranges.

The photonic crystal studied in our experiments consists of metallic pillars of diameter 80 μm arranged in a periodic hexagonal array of lattice constant 200 μm. The band structure calculations show an effective plasma frequency of $f_P = 1.02$ THz and a J point frequency of $f_J = 1.28$ THz. However, we note that these values are calculated with the neglect of losses within the metal. With losses included, it is no longer possible to define f_P, precisely because all wave vectors are of a complex nature, and there is no clear-cut demarcation between propagating and nonpropagating states. The inclusion of a loss term has the additional effect of reducing the value of f_J by a few percent. Details of the basic fabrication methods employed have been published elsewhere [16], but in brief, high-aspect-ratio polymer pillars are formed by backside UV exposure of SU-8 50 on a glass substrate, before being sputtered with gold. Because the gold thickness is greater than the electromagnetic radiation skin depth, the pillars behave in effect like solid metallic rods.

Figure 1(b) is a photograph of the photonic crystal together with superimposed arrows indicating the directions of the incident and negatively and positively refracted beams. A wave of frequency within the first band, and thus having parallel group velocity and wave vector, should undergo positive refraction, to emerge from the "positive refraction facet" (PRF) as indicated. Conversely, an incident wave of frequency within the second band, hence having antiparallel group velocity and wave vector, should experience negative refraction, emerging from the "negative refraction facet" (NRF), as predicted in [15].

Refraction of THz light by a photonic crystal can be experimentally measured using a conventional broadband spectrometer configured in an appropriate reflection geometry. Figure 2 illustrates the system used to measure the negatively refracted components of the incident broadband beam, while the positively refracted components were detected using a system whose second pair of parabolic mirrors and collection optics had been rotated clockwise by an angle of 120°. The THz radiation was generated using a photoconductive switch, fabricated on low temperature grown GaAs and detected electro-optically using a balanced scheme. The IR pulse used for generation and detection was produced from a Ti:sapphire laser of wavelength 780 nm, pulse duration 20 fs, average power 600 mW, and repetition rate

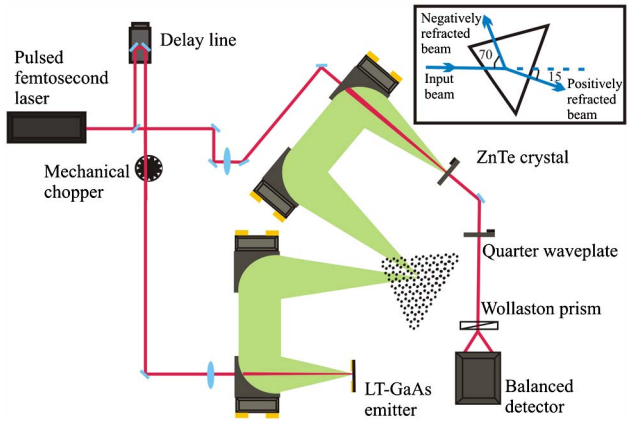

Fig. 2. (Color online) Schematic diagram of the reflection THz time domain spectrometer used to measure negative refraction. To measure positive refraction, the second pair of parabolic mirrors and detection optics were rotated through an appropriate angle. The inset shows the orientations of the two refracted beams relative to the incident and a (hypothetical) directly transmitted beams. For waves undergoing negative refraction, the beam emerging from the NRF forms an angle of about 70° with the incident beam, while for positive refraction, the exit beam is deflected by approximately 15° from the incident beam path. Therefore, the two beams are separated by an angle of the order of 120°.

76 MHz. After generation, the THz radiation was collected and focused onto the sample or a reflecting reference mirror (see below) using a pair of parabolic mirrors. Modeling [18] of the system shows that the best coupling of the incident wave to the refracted wave is provided for an incidence angle in the interval of 20°–30°, because the matching of the propagation constants in the structure and in the vacuum minimizes reflections of the beam at the sample interface. Therefore, in the experimental setup, an incidence angle of 25° was chosen. For both the cases of negative and positive refraction, a plane mirror placed at the THz beam focus allowed reference measurements to be undertaken to check the system alignment and performance. Another pair of parabolic mirrors, placed in an appropriate angular position, collected the radiation from the sample, which was then

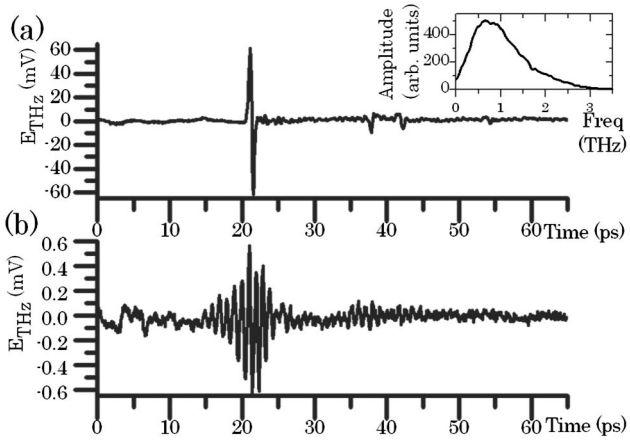

Fig. 3. (Color online) (a) Reference pulse in the time domain showing system performance. Inset, spectral content of this pulse. (b) THz pulse in the time domain that has interacted with the sample before emerging from the NRF.

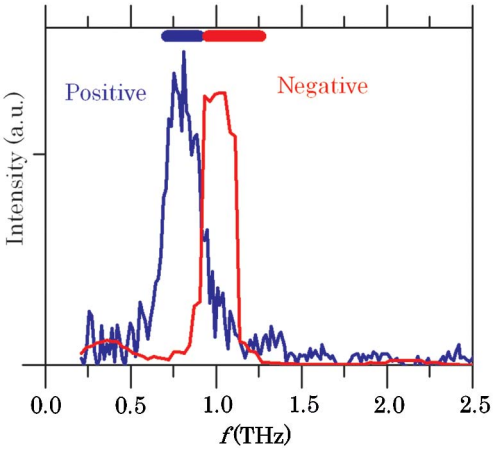

Fig. 4. (Color online) Spectral intensity of the two components of the THz pulse that are transmitted by the prism, corresponding to positive refraction when emerging from the PRF and negative refraction in the case of the NRF. The horizontal bars indicate the FWHM frequency ranges of the first (0.7–0.91 THz) and second (0.91–1.24 THz) photonic bands as determined experimentally.

focused onto the detector. It should be noted that the parabolic mirrors focused the broadband THz beam onto, and collected the narrowband refracted beam from, the sample over an angular range of approximately 10°—this is much smaller than the angular separation of the refracted beams.

Figure 3(a) shows the typical temporal dependence of the reference signal obtained from the spectrometer. The Fourier transform, which is shown in the inset, indicates a usable bandwidth of approximately 3 THz with maximum power being output around frequencies of 1 THz, which corresponds to the operating frequency of the device. Figure 3(b) shows the pulse that emerges from the NRF. Even though the amplitude is much reduced in the time domain, the negatively refracted pulse contains numerous oscillations. This pulse ringing is clear initial evidence that only a limited range of frequency components are steered by the device to emerge from the NRF. The THz beam emerging from the PRF is of a similar structure. The Fourier transforms of the pulses (Fig. 4) show the spectral content contained in both the negatively and positively refracted components of the original, incident THz beam, the rest being filtered away by the device.

It is clear that while there is some overlap of the tails of the spectral peaks, there are distinct passbands for the negatively and positively refracted waves, which correspond to the photonic bands having a positive and negative group velocity. The positive refraction band extends from 0.73 to 0.91 THz, while the negatively refracted band covers the spectral range of 0.91 to 1.24 THz, when defined by their FWHM. In both bands, approximately 10% of the incident beam power is refracted. The general form of these results is consistent with our theoretical band structure analysis, which should be recognized as being for a system consisting of an infinite array of pillars using a finite number of plane waves, whereas in the experiment a focused beam is incident on a finite structure. When losses are included, the value of f_P is no longer clear-cut and, as noted, losses also reduce the value of f_J, and both these trends are consistent with the experimental observations. Also, limitations on the micromachining processes used to construct the prism mean that the pillar diameters are somewhat more narrow toward their tops, and this will further reduce the predicted frequencies.

In summary, we have demonstrated, for the first time to our knowledge, the ability of a metallic photonic crystal prism to filter a broadband THz beam in such a way that two angularly resolved beams at different frequencies emerge. Essentially, the device works by positively refracting the frequency components in one interval and negatively refracting the frequency components in an adjacent interval by making use of the properties of the two lowest photonic bands of the crystal. It should also be noted that the top-hat shape of the transmission spectrum for the negatively refracted wave makes such a device attractive for use as a spectral filter.

This work was funded by the Engineering and Physical Science Research Council (EPSRC) of the United Kingdom through grant EP/C534263.

References and Notes

1. J. M. Chamberlain, Phil. Trans. R. Soc. Lond. A **362**, 199 (2004).
2. J. B. Jackson, M. Mourou, J. F. Whitaker, J. N. Duling III, S. C. Williamson, M. Menu, and G. A. Mourou, Opt. Commun. **281**, 527 (2008).
3. E. Pickwell and V. P. Wallace, J. Phys. D **39**, R301 (2006).
4. P. H. Siegel, IEEE Microwave Theory Tech. **50**, 910 (2002).
5. P. W. Milonni, *Fast Light, Slow Light and Left-Handed Light* (Taylor & Francis, 2005).
6. V. G. Veselago, Sov. Phys. Usp. **10**, 509 (1968).
7. D. O. S. Melville, R. J. Blaikie, and C. R. Wolf, Appl. Phys. Lett. **84**, 4403 (2004).
8. R. A. Shelby, D. R. Smith, and S. Schultz, Science **292**, 77 (2001).
9. P. V. Parimi, W. T. Lu, P. Vodo, J. Sokoloff, J. S. Derov, and S. Sridhar, Phys. Rev. Lett. **92**, 127401 (2004).
10. J. B. Pendry, Phys. Rev. Lett. **85**, 3966 (2000).
11. J. B. Pendry, D. Schurig, and D. R. Smith, Science **312**, 1780 (2006).
12. I. Newton, *Opticks: Or, a Treatise of the Reflexions, Refractions, Inflexions and Colours of Light* (William and John Innys, 1704).
13. S. Wang, F. Garet, K. Blary, E. Lheurette, J. L. Coutaz, and D. Lippens, Appl. Phys. Lett. **97**, 181902 (2010).
14. C. Luo, S. G. Johnson, J. D. Joannopolous, and J. B. Pendry, Phys. Rev. B **65**, 201104 (2002).
15. M. A. Kaliteevski, S. Brand, J. Garvie-Cook, R. A. Abram, and J. M. Chamberlain, Opt. Express **16**, 7330 (2008).
16. A. J. Gallant, M. A. Kaliteevski, S. Brand, D. Wood, M. C. Petty, R. A. Abram, and J. M. Chamberlain, J. Appl. Phys. **102**, 023102 (2007).
17. S. Brand, R. A. Abram, and M. A. Kaliteevski, Phys. Rev. B **B75**, 035102 (2007).
18. Finite-difference time-domain simulations to model the EM field profiles were carried out using the OmniSim software package.